Chinthalapudi et al., http://www.jcb.org/cgi/content/full/jcb.201404128/DC1

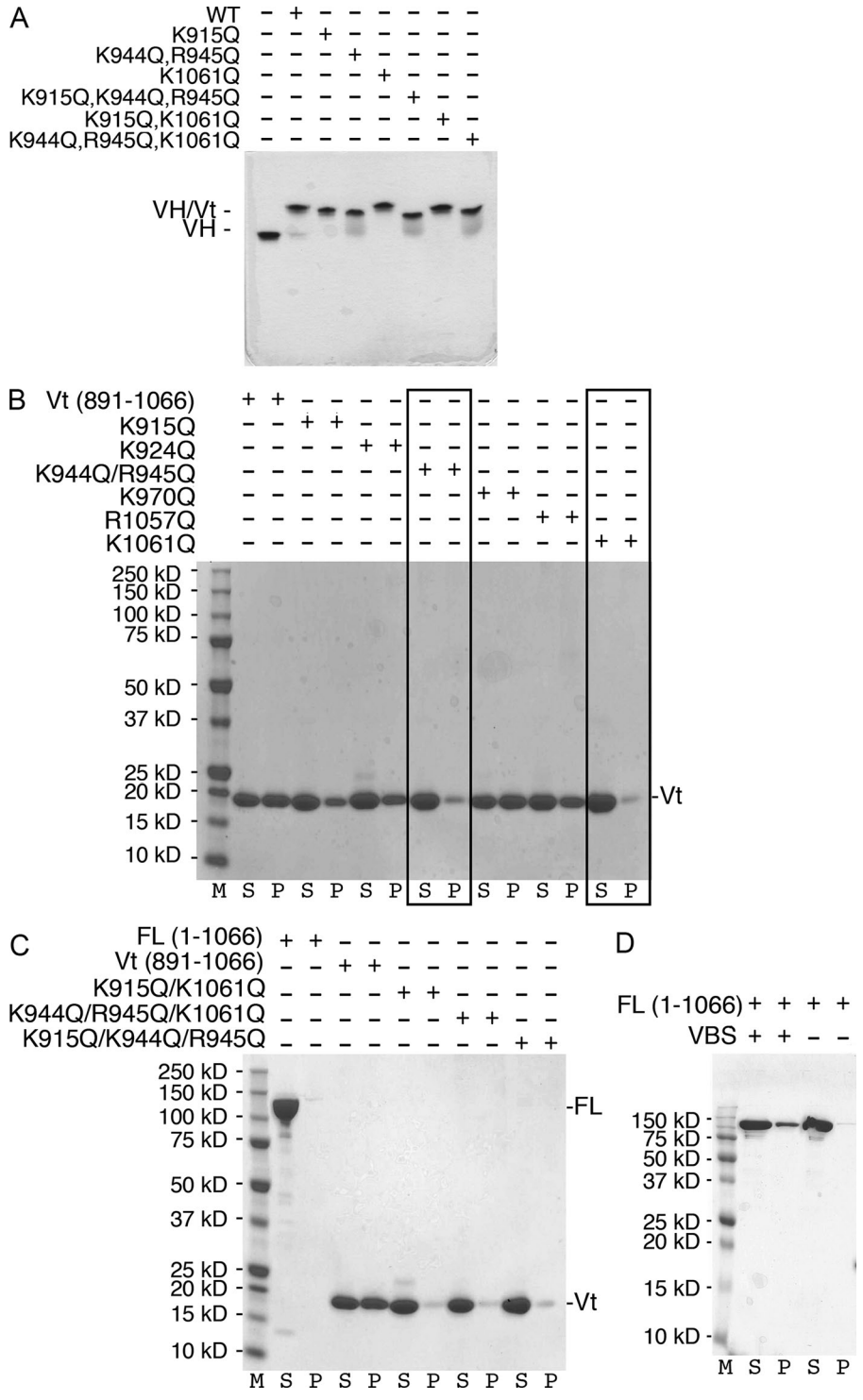

Figure S1. **Pull-down assay to analyze the lipid-binding capacity of vinculin.** (A) Vt mutants are capable of binding to VH (shown are the full gels of bands used in Fig. 2 A). The interaction of wild-type and mutant Vt with VH was analyzed by electrophoretic mobility shift assays on a native gel by incubating the respective Vt proteins with VH. (B–D) Pull-down assay to analyze the lipid-binding capacity of vinculin. Unilamellar vesicles of the phospholipids PC and PIP_2 were incubated with wild-type and mutant Vt (B: K915Q, K924Q, K944Q/R945Q, K970Q, R1057Q, and K1061Q; C: K915Q/K1061Q, K944Q/R945Q/K1061Q, and K915Q/ K944Q/R945Q) and sedimented. Supernatant (S) and pellet (P) fractions were detected on Coomassie-stained SDS-PAGE. Non-binding mutants K944Q/R945Q and K1061Q (boxed regions) were selected for further functional studies. (D) Inactive and talin-VBS (residues 1,945–1,970)-activated full-length (FL) vinculin were run as the nonbinding and binding controls, respectively. Cropped versions of these gels are shown in Fig. 2 B.

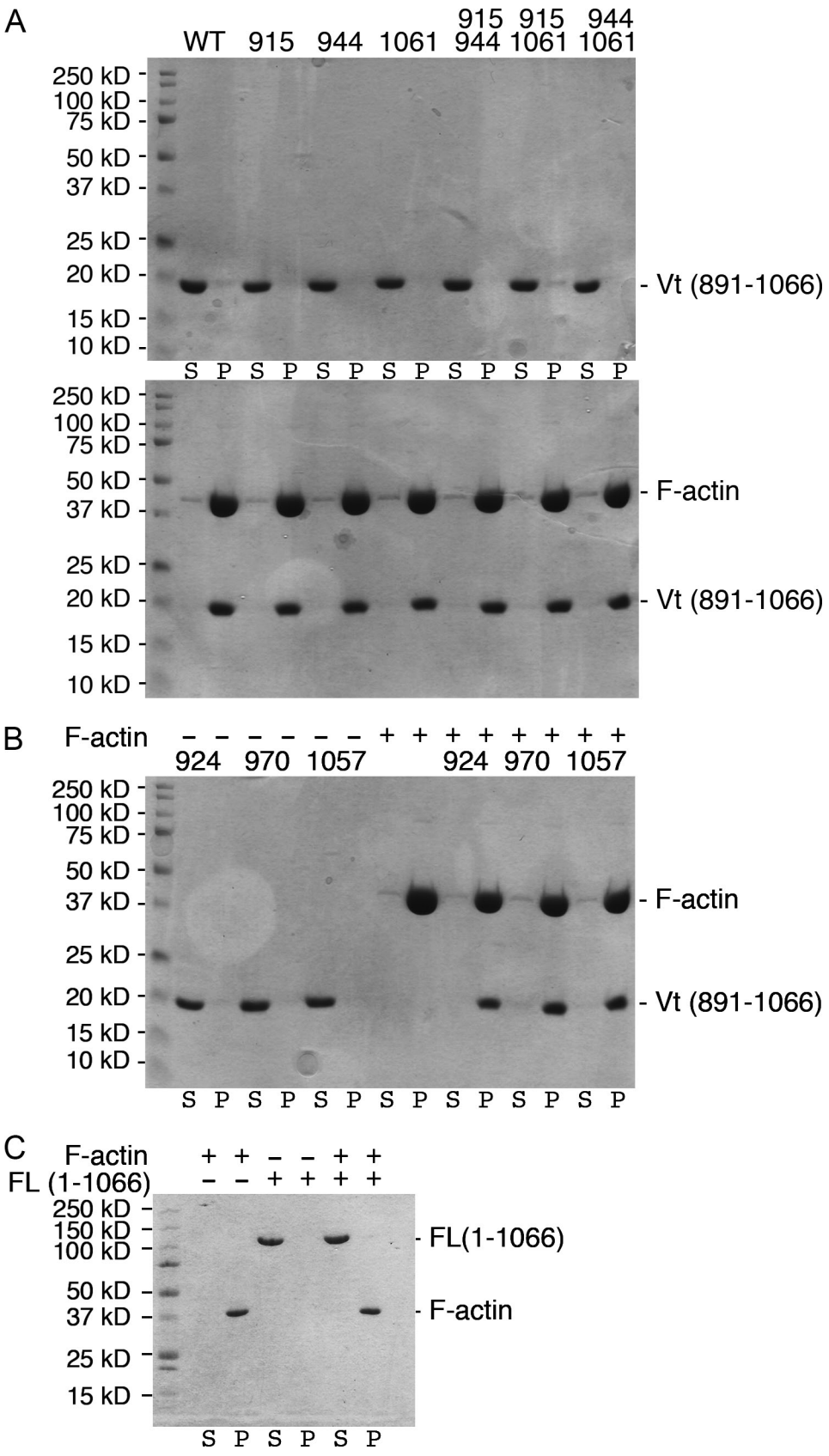

Figure S2. **Lipid-binding–deficient vinculin mutants cosediment with F-actin.** Wild-type and mutant Vt (A: K915Q, K944Q/R945Q "944," K1061Q, K915Q/K944Q/R945Q "915 944," K915Q/K1061Q, K944Q/R945Q/K1061Q "944 1061"; B: K924Q, K970Q, and R1057Q) were cosedimented with F-actin and analyzed on Coomassie-stained SDS-PAGE. Vinculin samples were also analyzed in the absence of F-actin (top gel in A and the first six lanes in B). S, Supernatant; P, pellet. (C) Full-length (FL) vinculin was run as the nonbinding control. Cropped versions of these gels are shown in Fig. 4 A.

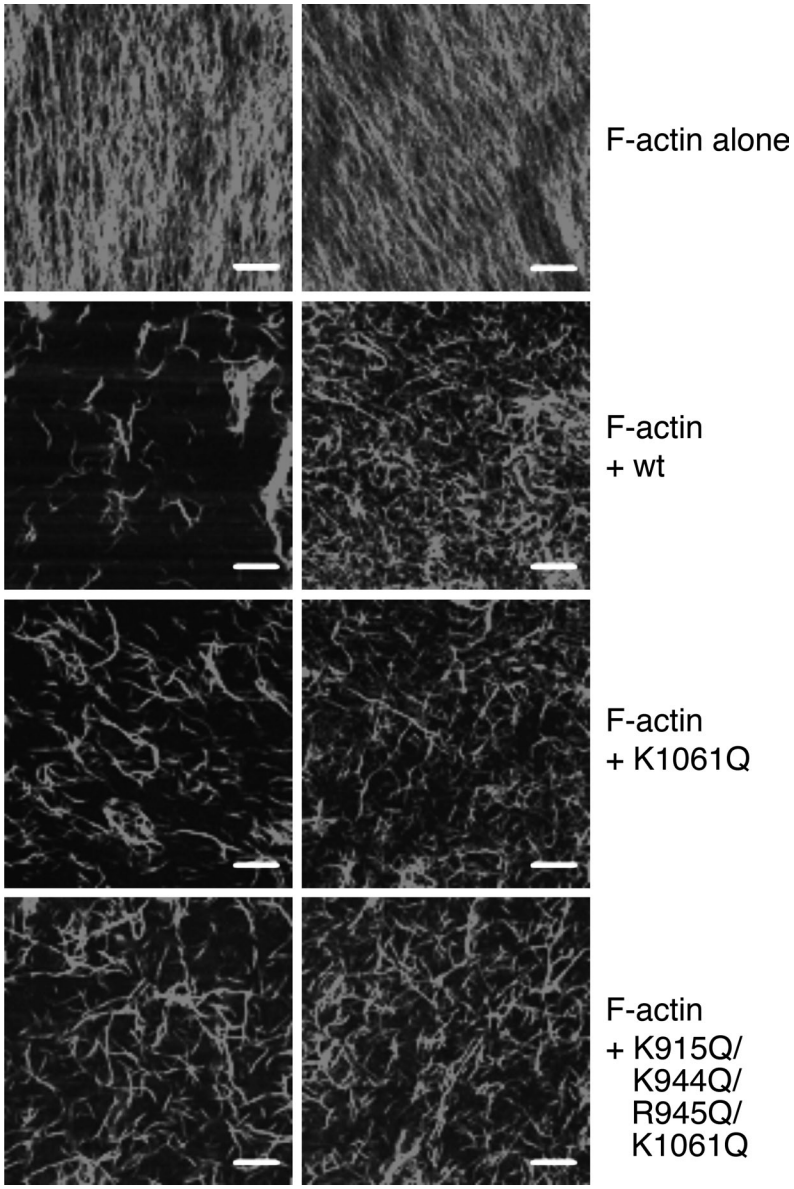

Figure S3. **Lipid-binding–deficient vinculin mutants bundle F-actin.** Confocal images of TRITC-phalloidin–labeled F-actin in the absence or presence of Vt (wild type, K1061Q mutant, or K915Q/K944Q/R945Q/K1061Q mutant) domain in Tris-HCl, pH 8.0 (left), or imidazole, pH 7.4 (right) buffers. Cropped versions of these micrographs are shown in Fig. 4 B. Bars, 20 µm.

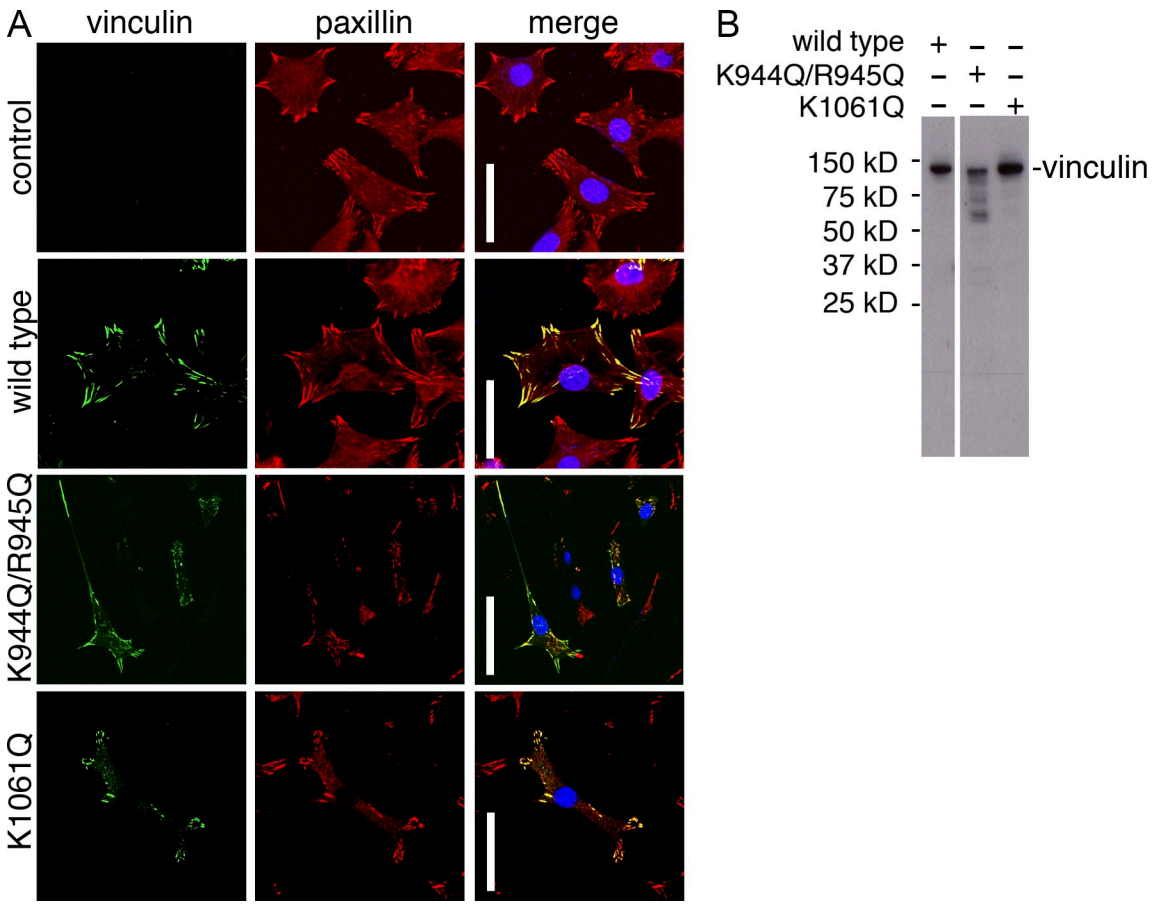

Figure S4. **PIP_2-directed oligomerization of vinculin contributes to the stabilization of FAs.** (A) *Vinculin*$^{-/-}$ MEFs engineered to express wild-type GFP-vinculin or mutant GFP-vinculin fusions (K944Q/R945Q and R1061Q) were analyzed by confocal laser scanning microscopy. MEFs were grown on fibronectin-coated cover slides, fixed after 24 h, and stained for paxillin with anti-paxillin primary and Alexa Fluor 568–conjugated secondary antibodies. Representative images, which define the localization of GFP-vinculin (green) and paxillin (red) at FAs, along with the merged channels, are shown. Also shown are nuclei stained with DAPI. Data shown are representative of three independent experiments. Bars, 50 µm. (B) The expression of wild-type and mutant forms of vinculin in reconstituted *vinculin*-null MEFs was determined by immunoblotting. Data shown are representative of three independent experiments.